Small, Potent, and Selective Diaryl Phosphonate Inhibitors for Urokinase-Type Plasminogen Activator with In Vivo Antimetastatic Properties

Jurgen Joossens,[†] Omar M. Ali,[†] Ibrahim El-Sayed,[†] Georgiana Surpateanu,[†] Pieter Van der Veken,[†] Anne-Marie Lambeir,[‡] Buddy Setyono-Han,[§] John A. Foekens,[§] Anneliese Schneider,[△] Wolfgang Schmalix,[△] Achiel Haemers,[†] and Koen Augustyns*,[†]

Laboratory of Medicinal Chemistry and Laboratory of Medical Biochemistry, University of Antwerp, Universiteitsplein 1, B-2610 Antwerp, Belgium, Erasmus MC, Josephine Nefkens Institute, Department of Medical Oncology, Dr. Molewaterplein 50, 3015 GE Rotterdam, Netherlands, and Wilex AG, Grillparzestr. 10, 81675 Munich, Germany

Received August 2, 2007

A set of small nonpeptidic diaryl phosphonate inhibitors was prepared. Some of these inhibitors show potent and highly selective irreversible uPA inhibition. The biochemical and modeling data prove that the combination of a benzylguanidine moiety with a diaryl phosphonate ester results in optimized molecules for derivatizing the serine alcohol in the uPA active site. Selected compounds show significant antimetastatic effects in the BN-472 rat mammary carcinoma model. We report in this paper a preclinical proof of concept that selective, irreversible uPA inhibitors could be valuable in antimetastatic therapy.

Introduction

Urokinase plasminogen activator (uPA[a]), a trypsin-like serine protease and its receptor (uPAR) are essential proteins in the proteolytic degradation process involved in cancer invasion and metastasis. uPA is selectively bound to the membrane-anchored uPAR and activates plasminogen into plasmin. Plasmin plays an important role in the breakdown of extracellular matrix (ECM). It activates several matrix metalloproteases, which in turn degrade several components of the ECM including fibrin, laminin, and fibronectin. Proteolytic degradation of this ECM is a key event in tumor invasion and metastasis. Recent data support uPA/uPAR as a valid therapeutic target.[1–3] An amidine-based, peptide-derived inhibitor (**1**) reduces the number of experimental lung metastases in a fibrosarcoma model in mice,[4] and two clinical phase I trials with uPA inhibitors **2a** (WX-UK1)[5] and its prodrug **2b** have been successfully completed (Figure 1).[6] Hence, uPA inhibition can be considered as a promising new noncytotoxic approach in cancer therapy to specifically block tumor metastasis in solid cancers.

Most of the published uPA inhibitors are reversible inhibitors.[7] Instead, we focus on irreversible uPA inhibition. Irreversible inhibition may have a stronger impact and will not lead to mechanism-based toxicity if selective. Moreover, the physiological role of the uPA system can be taken over by tissue plasminogen activator (tPA). tPA is a related trypsin-like serine protease which is also able to activate plasminogen but is known to be mainly involved in fibrinolysis. Indeed, uPA-deficient mice do not develop spontaneous phenotypic changes. This is also true for tPA-deficient mice but not for uPA/tPA or plasminogen deficient animals.[8] The development of selective inhibitors for uPA is hampered by its close resemblance to other trypsin-like serine proteases. Several inhibitors suffer from poor selectivity toward tPA, plasmin, or thrombin.[9] The latter enzyme is an important constituent of the blood coagulation cascade, and therefore, high selectivity is of utmost importance in the development of uPA inhibitors.

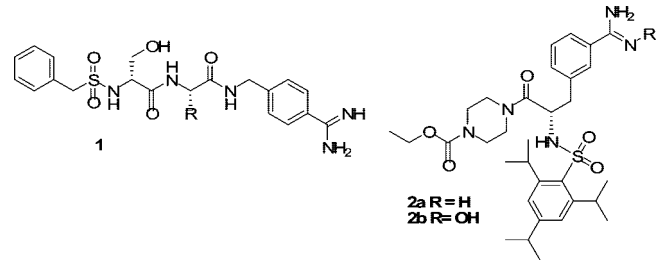

Figure 1. uPA inhibitor **1** is active in an in vivo tumor model, and inhibitors **2** are in phase 1 clinical trials.

We recently reported the first irreversible, selective, and potent diphenyl phosphonate peptidic inhibitors for uPA.[10] These inhibitors were designed using *Z*-D-Ser-Ala-Arginal **3** (Figure 2) as a lead compound.[11] The aldehyde function was substituted for a diphenyl phosphonate group (**4**), which is known to react in a covalent way with the active site serine of serine proteases, affording a phosphonylated and irreversibly inhibited enzyme.[12,13] In a next step the P1 position was optimized by substituting the arginine moiety for various linear or cyclic guanidinylated side chains.[14] A benzylguanidine afforded the most interesting compounds (**5**), providing high selectivity and high potency toward uPA.[10]

These inhibitors were further optimized at the P4 position. Several amide and sulfonamide groups were linked to the terminal amino group.[11,15,16] The best compounds showed inhibitory activities in the low nM range in specific assay conditions and remarkable in vitro selectivity indices reflecting ratios of inactivation rates of 3000 or more toward related enzymes from the fibrinolytic and blood coagulation systems. Compounds within series **5** belong to the most potent and selective uPA inhibitors reported.[16] Release of cytotoxic phenol upon covalent binding to the target protein constitutes a potential problem in biological settings using diphenyl phosphonates. To circumvent this problem, a diaryl phosphonate containing a "safe" phenol, *p*-acetylaminophenol (paracetamol) was prepared.[16]

* To whom correspondence should be addressed. Tel.: +32-3-8202703. Fax: +32-3-8202739 . E-mail: koen.augustyns@ua.ac.be.

[†] Laboratory of Medicinal Chemistry, University of Antwerp.

[‡] Laboratory of Medical Biochemistry, University of Antwerp.

[§] Erasmus MC, Josephine Nefkens Institute.

[△] Wilex AG.

[a] Abbreviations: uPA, urokinase-type plasminogen activator; tPA, tissue-type plasminogen activator; uPAR, urokinase-type plasminogen activator receptor; FXa, factor Xa; ECM, extracellular matrix.

10.1021/jm700962j CCC: $37.00
Published on Web 12/01/2007

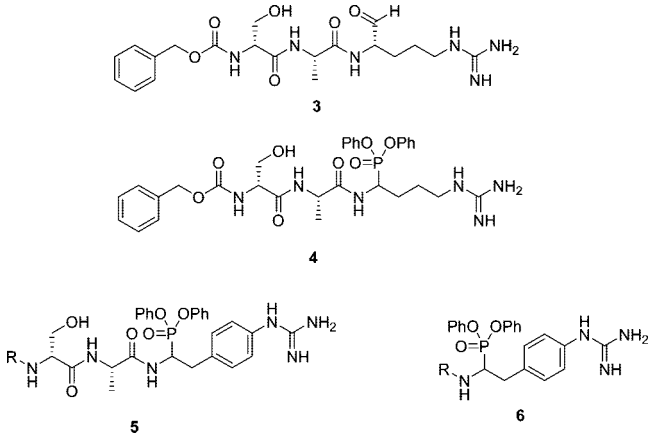

Figure 2. Development of small nonpeptidic irreversible uPA inhibitors. 1. Conversion of the lead arginal peptide **3** into an irreversible inhibitor **4**. 2. Optimization of selectivity and activity. A benzylguanidine is important for activity and selectivity and the R group is important for selectivity toward uPA (**5**). 3. Nonpeptidic, small, potent, and selective uPA inhibitors **6**.

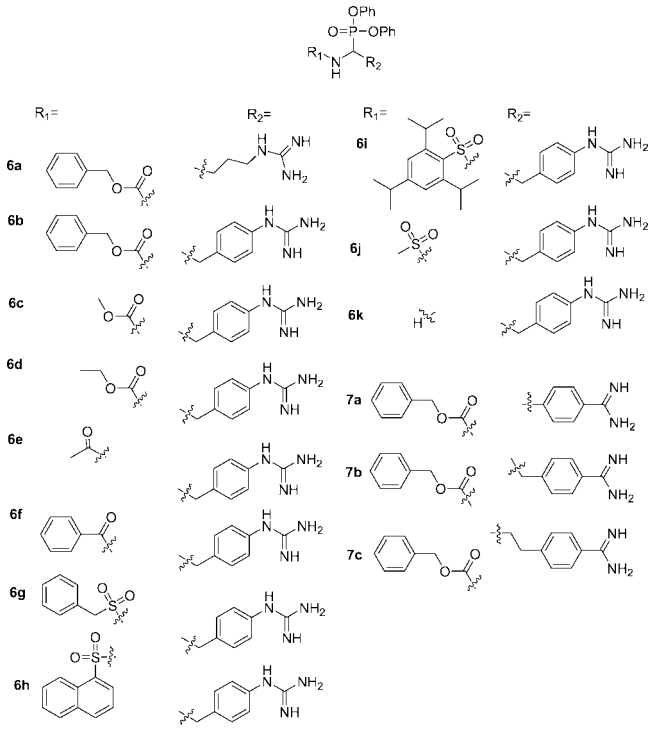

Figure 3. Structures of diphenyl phosphonates **6** and **7**.

In this paper, we report a further improvement of the drug-like properties of these compounds. We found that substituting the peptide tail for a small group (**6**) did not change the uPA inhibitory activity nor the selectivity versus other trypsine-like proteases. The influence of different substituents on the α-amino group was investigated (Figure 3, **6b–k**). The guanidinylated compounds were compared with their amidine analogues (**7a–c**). Finally, some di(4-acetamidophenyl)phosphonates were prepared (Figure 4, **8a–c**). Based on the activity−selectivity profile and some physicochemical properties, two compounds were selected for evaluation of their antitumor and antimetastatic properties in a rat mammary carcinoma model. During the course of our investigation,[17] Oleksyszyn et al. also reported the uPA inhibitory activities of **6a**, **6b**, and **7a**, confirming our uPA inhibition results.[18,19] In contrast to the group of Oleksyszyn, we decided not to publish preliminary data. Our more elaborated study has

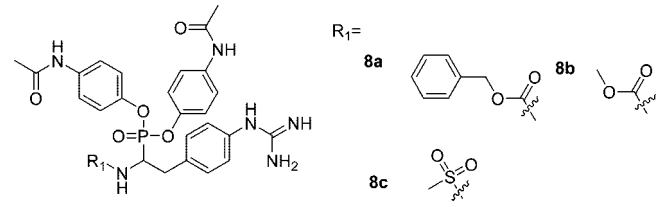

Figure 4. Structures of di-4-acetamidophenyl phosphonates **8**.

Scheme 1. Synthesis of the Inhibitors[a]

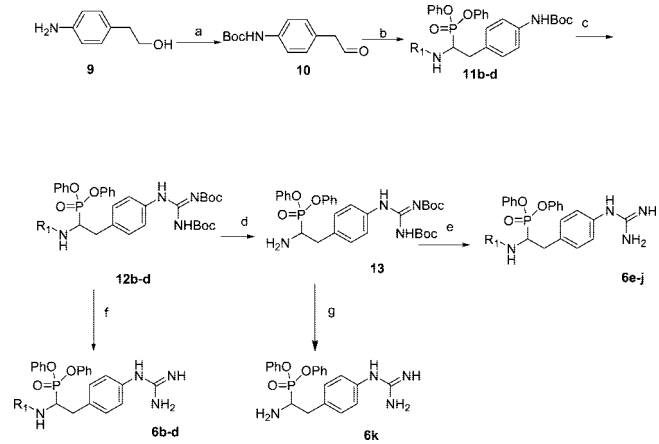

[a] Reagents and conditions: (a) (i) di-*tert*-butyl dicarbonate, TEA, dioxane; (ii) Dess−Martin oxidation; (b) benzyl carbamate, triphenyl phosphite, $Cu(OTf)_2$, CH_2Cl_2; (c) (i) trifluoroacetic acid; (ii) *N*,*N*′-bis(tert-butoxycarbonyl)-1-guanylpyrazole, MeCN; (d) (for **12b**) H_2, Pd/C, MeOH; (e) (i) R_2-Cl, pyridine; (ii) trifluoroacetic acid; (f) trifluoroacetic acid, CH_2Cl_2.

led to more potent and selective compounds than previously reported. Also, in this paper we report for the first time in vivo antimetastatic properties of diaryl phosphonate uPA inhibitors.

Chemistry. The synthesis of diphenyl phosphonates **6** is shown in Scheme 1. Boc-protected 4-aminophenylacetaldehyde (**10**), prepared from the corresponding alcohol (**9**) with Dess−Martin periodinane[20] was used as starting material. An amidoalkylation reaction with the corresponding carbamate and triphenylphosphite, using copper triflate as catalyst, afforded the diphenyl phosphonates **11b–d**.[21] After acidolytic removal of the Boc protecting group, *N*,*N*′-bis(*tert*-butoxycarbonyl)-1-guanylpyrazole was used to introduce the protected guanidine group (**12b–d**). Final compounds **6b−d** were obtained after deprotection with trifluoroacetic acid. Deprotection of **12b** under hydrogenolytic conditions (**13**) and Boc deprotection resulted in **6k**. Acylation or sulfonylation of **13** and subsequent deprotection afforded compounds **6e–j**. The di(4-acetamidophenyl) phosphonates **8** were prepared analogously using tri-4-acetylaminophenylphosphite and $TiCl_4$.

Amidine compounds **7** were synthesized using the corresponding cyanoaldehydes (**15**, Scheme 2) in an amidoalkylation reaction, followed by conversion to the amidine with a Pinner reaction.[22,23]

Biochemical Evaluation. IC_{50} values of compounds **6–8** were determined for uPA and for other representative trypsin-like serine proteases (Table 1).[10,16] The latter are involved in the blood coagulation cascade and fibrinolysis: tPA, plasmin, thrombin, and FXa.

Comparison of compounds **6** with different α-amino substituents shows that the highest potency as uPA inhibitor is obtained when there is no steric hindrance close to the α-amino group. Bulky substituents such as in compounds **6h** and **6i** are not favorable. The best activity−selectivity profile is observed when

Scheme 2. Synthesis of Inhibitors **7a–c**[a]

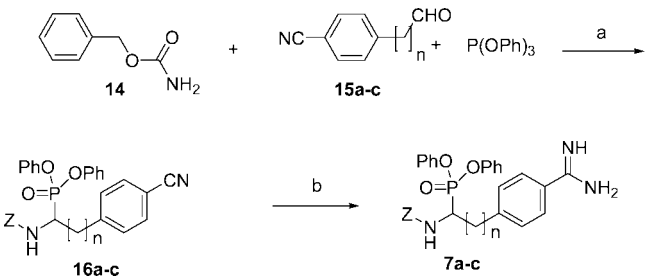

[a] Reagents and conditions: (a) $Cu(OTf)_2$, CH_2Cl_2 (b) (i) MeOH/$CHCl_3$ (1:1), $HCl_{(g)}$ (ii) 2 M NH_3 in EtOH, $n = 0$ to 2.

small groups are introduced such as in methylcarbamate **6c**, acetamide **6e**, and methylsulfonamide **6j**. The free amine (**6k**) is nearly 1000 times less-active.

The importance of the diphenyl phosphonate group in this benzylguanidine series to obtain potent and selective nonpeptidic inhibitors is highlighted in Figure 5. Omitting the peptide part in **17**,[24] a potent and selective inhibitor without serine protease warhead, decreases the uPA inhibitory activity about 1000-fold (**18**).[25] On the contrary, comparing the activity of **6b** with its corresponding peptide **5** (R = benzylsulfonyl)[16] shows no significant decrease in uPA inhibition, and the small inhibitor is even more selective for uPA. The importance of the benzylguanidine group is demonstrated upon comparison of **6a** and **6b**. A small diphenyl phosphonate inhibitor with benzylguanidine side chain (**6b**) is about 100-fold more potent and far more selective than the corresponding compound with an arginine-like side chain (**6a**). The observation that the arginal warhead in **3** is only active in a peptide structure confirms the importance of our combination of a diphenyl phosphonate with a benzylguanidine.[10,11]

As already shown for peptidic inhibitors, the diphenyl phosphonate ester can be substituted for a di-4-acetamidophenyl ester without loss of potency. The selectivity profile is somewhat less favorable but these compounds (**8a**−**c**) are still highly selective. Amidines (**7a**−**c**) are less favorable as irreversible uPA inhibitors.

Compound **6c** (UAMC-00150) and its paracetamol analogue **8b** (UAMC-00251) were selected as the most promising compounds for further investigation. Compound **6c** shows the lowest IC_{50} value and the best selectivity profile. Moreover, the synthetic route is short, with a good overall yield.

Modeling Study. A molecular modeling study was performed to offer a molecular basis for the high potency and remarkable selectivity of the here reported nonpeptidic uPA inhibitors. The same methodology as already reported was used.[16] We presume that the highly specific interactions of the benzylguanidine in the S1 pocket place the diaryl phosphonate group at the optimal position for a covalent reaction with the alcohol of Ser195 (Figure 6). Therefore, the extra interactions observed between the peptidic part of **5** and uPA are not necessary for a good and selective interaction with uPA.

Further Evaluation of Compounds 6c and 8b. Compounds **6c** and **8b** were further evaluated to determine the feasibility of using them for in vivo evaluation (Table 2). Because these compounds are designed with an electrophilic phosphonate warhead for covalent interaction with the serine alcohol in the active site, their stability might be compromised. However, they exhibited excellent stability at different pH values, for example, more than 2.5 days at pH 7.4. As expected, **6c** and **8b** are less stable at basic pH, and the instability of the paracetamol analogue **8b** is slightly higher. Furthermore, the plasma stability of both compounds is more than acceptable, with more than 60% parent compound left after 3 h incubation at 37 °C. Stability in the stock solutions used in the in vivo assays was confirmed. $LogD_{7.4}$ and the solubility also reflect their drug-like properties. These compounds showed low cytotoxicity in an epithelial cell line of Brown Norway rats (BN-175, unpublished data).

Compounds **6c** and **8b** were also tested as inhibitors of rat and mouse enzymes. Both compounds showed low nM IC_{50} values (<25 nM) for rodent uPA and μM IC_{50} values for rodent plasmin and thrombin. The activity against rodent enzymes confirmed the suitability of these uPA inhibitors to be used in vivo in rodent tumor models.

Efficacy Study in the BN472 Mammary Rat Tumor Model. The objective of this study was to investigate the antitumor and antimetastatic efficacy of the irreversible uPA-inhibitors **6c** and **8b** in Brown Norwegian rats bearing BN-472 rat mammary tumors. In breast cancer, it is established that high expression levels of uPA, its cellular receptor (uPAR), and its inhibitor (PAI-1) support invasion, metastatic spread, and neoangiogenesis of tumors and strongly correlate with poor patient prognosis. The BN-472 metastasizing mammary tumor that grows in Brown Norwegian rats expresses a significant amount of uPA, uPAR, and PAI-1 as assessed by real-time RT-PCR analysis and represents an excellent in vivo model to study the efficacy of newly designed drugs that interfere in the uPA-system of plasminogen activation.[5]

Tumors implanted orthotopically were allowed to grow for three days. Starting on day 4 after tumor inoculation, **6c** and **8b** were administered i.p. daily for 17 to 18 days at 0.1 and 1 mg/kg. Control animals were treated i.p. with vehicle only. End points of this study were the evaluation of antitumor effects (measured by tumor size and tumor weight, Figure 7), antimetastatic effects (measured by number of lung foci and weight of axillary lymph nodes, Figure 8), and side effects (measured by body weight and weight of several organs).

Daily administration of **6a** and **8b** at 0.1 mg/kg and 1 mg/kg resulted in significant inhibition of tumor growth in the range of 10–18% considering the end point tumor size. The decrease in tumor weight was 9–27% though the effect in the **8b** low-dose group was statistically not significant. The antitumor effect was not dose-dependent.

The antimetastatic effect observed by a decrease in the number of lung foci (29–70%) and the weight of axillary lymph nodes (46–73%) was statistically significant in all compound and dose groups except for 0.1 mg/kg of **6c** in the end point axillary lymph node weight. The antimetastatic effect was dose-dependent in both **6c** and **8b** groups.

The moderate in vivo antitumor activity with an up to 27% inhibition in tumor weight falls within the range of 22–56% observed previously in independent experiments with the uPA-inhibitor **2a** that was applied daily by subcutaneous or intraperitoneal administration in the same tumor model.[5] The antimetastatic activity of up to 73% was more pronounced and was also similar to the up to 62% inhibition observed previously following daily administrations of compound **2a**.[5] The higher antimetastatic activity compared to the antitumor activity was expected based on the function of uPA in tumor invasion and metastasis. The Spearman rank correlations between primary tumor weight and the metastatic end points were not statistically significant (r_s= 0.19, $n = 90$, for the axial lymph node weight; r_s=0.03, $n = 90$, for the number of lung foci), suggesting that the irreversible uPA-inhibitors independently exert both anti-

Table 1. Inhibitory Activities against uPA and Related Enzymes

			IC$_{50}$ (μM) or % inhibition at given concentration (μM)			
	IC$_{50}$ (nM) uPA	k_{app}($M^{-1}.s^{-1}$) uPA	tPA	plasmin	thrombin	FXa
6a	840 ± 200[a]	$10 \times 10^1 \pm 6 \times 10^1$[b]	44 ± 20 (50)[c]	30 ± 2 (35)	0.78 ± 0.04 (0.9)	70% at 250
6b	7 ± 2	$42 \times 10^3 \pm 3 \times 10^3$	12.0 ± 0.8 (1700)	3.0 ± 0.6 (300)	2.4 ± 0.4 (300)	100 ± 20 (11000)
6c	3.1 ± 0.5	$62 \times 10^3 \pm 4 \times 10^3$[b]	23 ± 6 (7000)	13 ± 2 (4300)	17.0 ± 2.3 (5600)	57% at 250
6d	8 ± 3	$40 \times 10^3 \pm 20 \times 10^3$[b]	57 ± 14 (7000)	16 ± 3 (2000)	3.8 ± 0.2 (500)	62% at 250
6e	7.2 ± 0.6	$14 \times 10^5 \pm 0.2 \times 10^5$	36.6 ± 2.2 (3700)	57 ± 1.3 (5700)	32.2 ± 1.4 (3200)	37% at 250
6f	114 ± 11	$24 \times 10^2 \pm 12 \times 10^2$[b]	125 (1000)	14 ± 1 (120)	65% at 125	>250
6g	7.7 ± 0.7	$19 \times 10^3 \pm 1 \times 10^3$	7.3 ± 0.5 (1000)	17 ± 2 (2000)	11.9 ± 1.7 (1500)	59% at 62
6h	26.5 ± 1.4	$73 \times 10^2 \pm 4 \times 10^2$	44 ± 10 (1600)	1.2 ± 0.1 (40)	8.1 ± 0.8 (300)	27 ± 2 (1000)
6i	260 ± 30	$16 \times 10^2 \pm 1 \times 10^2$	16 ± 1 (60)	~125 (500)	60% at 250	20 ± 2 (80)
6j	6.6 ± 0.8	$14 \times 10^4 \pm 1 \times 10^4$	8 ± 2 (1000)	11 ± 1 (1600)	~125 (19000)	~250 (40000)
6k	1600 ± 130	NA	32% at 250	31% at 250	41% at 250	11% at 250
7a	60000 ± 10000	$43 \times 10^0 \pm 6 \times 10^0$	66 ± 7 (1)	3.6 ± 0.4	0.288 ± 0.006	6.0 ± 0.2
7b	67 ± 25	$20 \times 10^2 \pm 1 \times 10^2$[b]	4 ± 2 (60)	1.2 ± 0.1 (20)	20 ± 2 (300)	65% at 250
7c	900 ± 80	$14 \times 10^1 \pm 1 \times 10^1$	68 ± 9 (70)	6.2 ± 0.4 (7)	17 ± 2 (20)	13.7 ± 1.3 (15)
8a	4.2 ± 0.9	$80 \times 10^3 \pm 5 \times 10^3$[b]	7 ± 1 (1700)	0.9 ± 0.2 (200)	0.39 ± 0.03 (90)	100 ± 24 (23000)
8b	3.4 ± 0.4	$10.00 \times 10^5 \pm 0.03 \times 10^5$	6.1 ± 0.7 (1800)	2.8 ± 0.5 (800)	1.13 ± 0.06 (300)	30 ± 6 (9000)
8c	3.5 ± 0.5	$21 \times 10^4 \pm 1 \times 10^4$	3.7 ± 0.4 (1000)	2.0 ± 0.4 (550)	2.35 ± 0.06 (700)	55% at 250

[a] Standard error on the fit. [b] Compound showed a two-step mechanism, k_{app}, calculated as k_2/K_1. [c] Selectivity index: IC$_{50}$/IC$_{50}$ uPA.

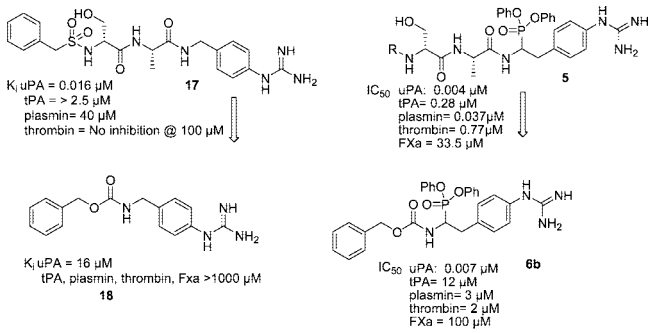

Figure 5. The small irreversible diphenyl phosphonate uPA inhibitor **6b** remains nearly equally potent and selective compared to the peptidic analogues **5** (R = benzylsulfonyl) and **17**. This is not true for the small reversible uPA inhibitor **18**. R = α-toluenesulfonyl.

tumor and antimetastatic activities and suggesting that the antimetastatic effects are not secondary to an effect on tumor growth.

Daily observations during the whole treatment period of 17 to 18 days showed that both compounds were generally well-tolerated. The body weight and the weight of different organs of the animals were not affected by the treatment.

In conclusion, these results obtained with **6c** and **8b** show for the first time that irreversible and selective uPA inhibitors exert moderate effects on the primary tumor but are highly active in the inhibition of metastatic development. These experiments confirm the data obtained with reversible uPA inhibitors[4,5,24] and prove the importance of uPA as target in the design of antimetastatic drugs.

Conclusion

We developed a series of small irreversible uPA inhibitors from previously reported peptidic diaryl phosphonates. Remarkably, removal of the peptidic tail did not influence potency nor selectivity and resulted in irreversible uPA inhibitors with nanomolar potency and more than 1000-fold selectivity over highly related proteases. Two compounds of this series were further evaluated for their suitability to be used in rodent tumor models. We have shown for the first time that irreversible uPA inhibitors exhibit promising antimetastatic properties in a rat mammary carcinoma model without any signs of acute toxicity.

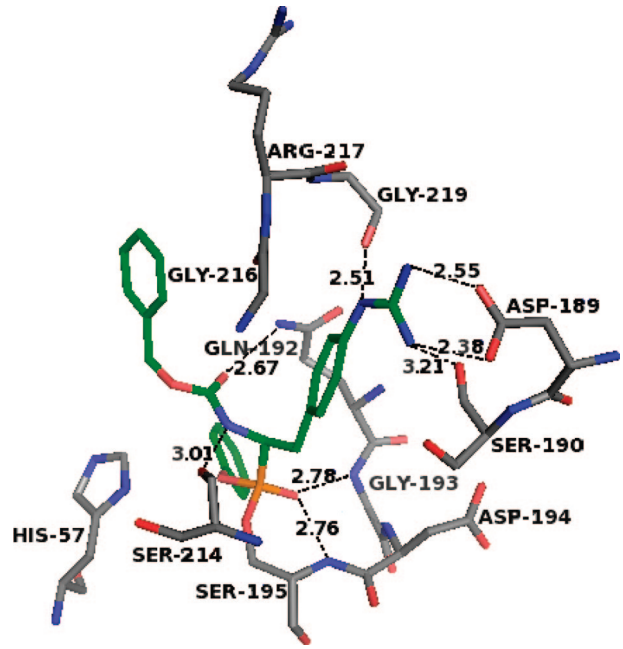

Figure 6. Inhibitor **6b** modeled in the active pocket of uPA after reaction with the alcohol of Ser195. (Carbons of the inhibitor are green, carbons of uPA are gray, nitrogens are blue, oxygens are red, phosphorus are orange. Ionic and hydrogen bonds are shown with dotted lines and their distances are shown in Å.) The terminal guanidine ion is deeply inserted into the S1 pocket, and this guanidine group forms the typical symmetrical salt bridge to the carboxylate of Asp189. Furthermore, one nitrogen atom makes a hydrogen bond with the carbonyl oxygen of Gly219, and another nitrogen atom forms a hydrogen bond with the alcohol of Ser190. The phenyl ring of the benzylguanidine is sandwiched between the planes of the amide bonds of Trp215−Gly216 and Ser190−Cys191 and is placed in a hydrophobic region of the active site. The phosphonate oxygen binds into the oxyanion hole, making hydrogen bonds to the backbone NH groups of Gly193 and Ser195. The α-amino nitrogen interacts with the backbone carbonyl of Ser214, and the carbonyl oxygen of the carbamate forms a hydrogen bond with the side chain of Gln192. The phenyl ring of the remaining phenol is placed in the hydrophobic S1′ pocket.

This further validates uPA as an interesting target in the design of antimetastatic drugs.

Experimental Section

Reagents were obtained from Sigma-Aldrich or Acros. Characterization of all compounds was done with ^{1}H NMR and mass

Table 2. Further Evaluation of **6c** and **8b**

property	6c	8b
LogD (pH 7.4)	1.1	−0.08
apparent solubility[a]	>200 μM	>200 μM
$t_{1/2}$, pH 1 (37 °C)	>2 weeks	35 h
$t_{1/2}$, pH 4 (37 °C)	>2 weeks	>2 weeks
$t_{1/2}$, pH 7.4 (37 °C)	5 days	64 h
$t_{1/2}$, pH 8.8 (37 °C)	6 h	3 h
plasma stability (37 °C)[b]	63% at 3 h	81% at 3 h
IC_{50} rat-uPA (μM)	0.0195	0.0245
IC_{50} mouse-uPA (μM)	0.032	0.008
IC_{50} rat-plasmin (μM)	15	2.2
IC_{50} mouse-plasmin (μM)	25	4.8
IC_{50} rat-thrombin (μM)	>100	45
IC_{50} mouse-thrombin (μM)	42	4.5

[a] In 2% DMSO in PBS, pH 7.4. [b] The % parent compound left.

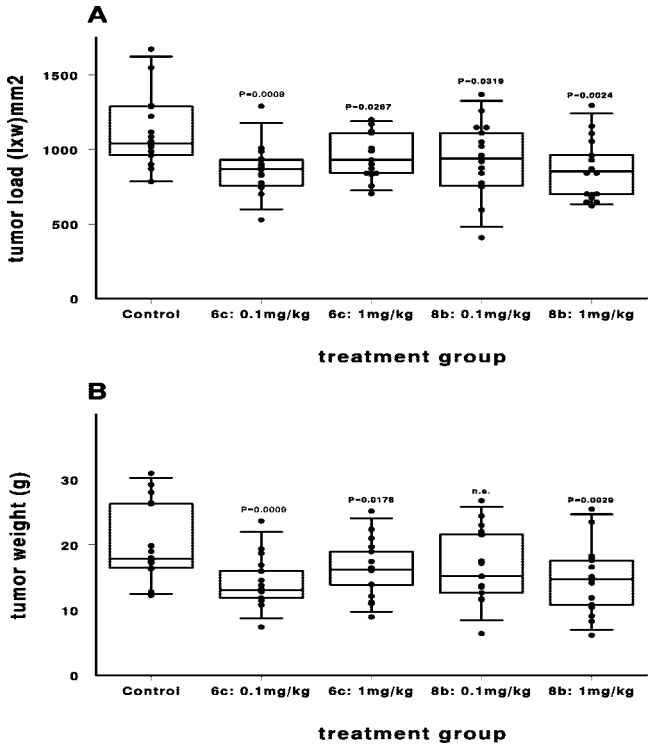

Figure 7. Effects of compounds **6c** and **8b** on primary tumor size and weight in rats bearing BN472 breast tumors. Compounds **6c** and **8b** were administered i.p. daily during days 17–18 at 0.1 and 1 mg/kg, starting on day 4 after tumor inoculation. Control animals were treated i.p. with vehicle only. Comparisons of the tumor sizes and weights at the end of the treatment period are presented as Box-Whisker graphs. The boxes show the median, the 25th and 75th percentiles are indicated as horizontal lines, the whiskers indicate the 5th and 95th percentile ranges, and the dots represent all the individually observed values. The unadjusted level for statistical significance was $P = 0.05$ when comparing treatment groups vs control (n.s. = not significant).

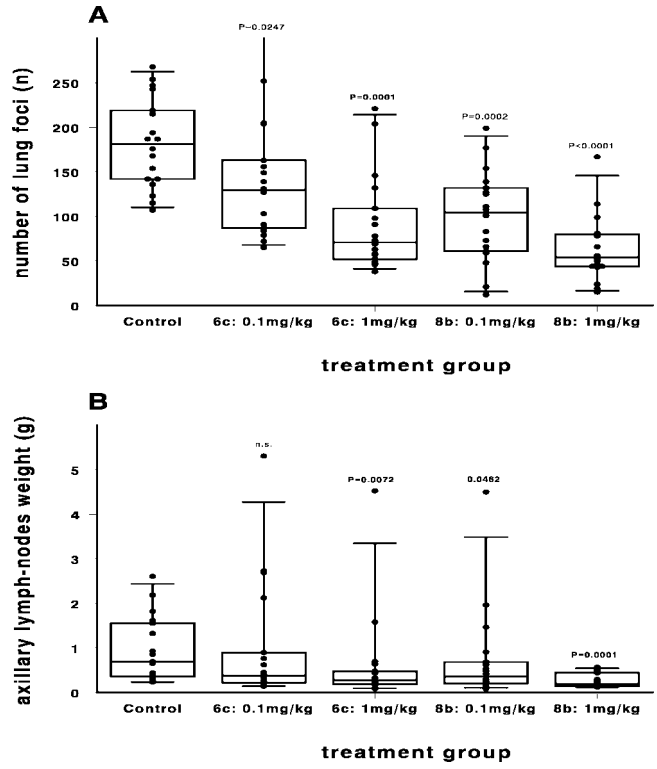

Figure 8. Antimetastatic effects of compounds **6c** and **8b** are measured by number of lung foci and axillary lymph node weight in rats bearing BN472 breast tumors. Compounds **6c** and **8b** were administered i.p. daily during days 17–18 at 0.1 and 1 mg/kg, starting on day 4 after tumor inoculation. Control animals were treated i.p. with vehicle only. Comparisons of the number of lung foci and the weight of axillary lymph nodes at the end of the treatment period are presented as Box-Whisker graphs. The boxes show the median, the 25th and 75th percentiles as horizontal lines, the whiskers indicate the 5th and 95th percentile ranges, and the dots represent all the individually observed values. The unadjusted level for statistical significance was $P = 0.05$ when comparing treatment groups vs control (n.s. = not significant).

spectrometry. ^{1}H NMR spectra were recorded on a 400 MHz Bruker Avance DRX-400 spectrometer. ES mass spectra were obtained from an Esquire 3000plus iontrap mass spectrometer from Bruker Daltonics. Purity was verified using two diverse HPLC systems using, respectively, a mass and UV-detector. Water (A) and CH_3CN (B) were used as eluents. LC-MS spectra were recorded on an Agilent 1100 Series HPLC system using a Alltech Prevail C18 column (2.1 × 50 mm, 3 μm) coupled with an Esquire 3000plus as MS detector and a 5–100% B, 20 min gradient was used with a flow rate from 0.2 mL/min. Formic acid 0.1% was added to solvents A and B. Reversed phase HPLC was run on a Gilson instrument equipped with an Ultrasphere ODS column (4.6 × 250 mm, 5 μm). A 10–100% B, 35 min gradient was used with a flow rate from 1 mL/min. Trifluoroacetic acid 0.1% was added to solvent A and B. A wavelength of 214 nm was used. When necessary, the products were purified with flash chromatography on a Flashmaster II (Jones chromatography), with a 30 min gradient of 0–50% EtOAc in hexane or 0–25% MeOH in EtOAc. The synthesis of compounds **10**, **11b**, **12b**, **13**, **6a**, **6b**, **15a**–**b**, **16a**,**b**, and tri-4-acetamidophenyl phosphite was already reported.[10,12,16] Slightly modified procedures for **10**, **11b**, **12b**, **13**, and tri-4-acetamidophenyl phosphite are placed in the Supporting Information.

Methyl 1-(Diphenoxyphosphoryl)-2-(4-(*tert*-butyloxycarbonylamino)phenyl)ethyl-carbamate (11c). To a solution of crude aldehyde **10** (1 equiv),[10,16] triphenyl phosphite (1 equiv), and methyl carbamate (1 equiv) in 50 mL CH_2Cl_2, 0.1 equiv $Cu(OTf)_2$ was added. The solution was stirred at room temperature for 4 h. CH_2Cl_2 was removed in vacuo. The crude product was dissolved in MeOH and the solution was kept at 4 °C until precipitation of diphenyl phosphonates was complete. Yield 63%; ^{1}H NMR ($CDCl_3$) δ 1.5 (s, 9H), 3.0–3.4 (m, 2H), 3.1 (s, 3H), 4.7 (m, 1H), 6.5 (s, 1H), 7.1–7.4 (m, 14H); MS (ESI) *m*/*z* 549 $[M + Na]^+$.

Ethyl 1-(Diphenoxyphosphoryl)-2-(4-(*tert*-butyloxycarbonylamino)phenyl)ethyl-carbamate (11d). Same procedure as for **11c**. Yield 57%; ^{1}H NMR ($CDCl_3$) δ 1.3 (t, 3H), 1.5 (s, 9H), 3.0–3.4 (m, 2H), 4.1 (q, 2H), 4.7 (m, 1H), 5.1 (m, 1H), 6.5 (s, 1H), 7.1–7.6 (m, 12H); MS (ESI) *m*/*z* 563 $[M + Na]^+$.

Methyl 2-(4-(*N*,*N*′-Bis(*tert*-butyloxycarbonyl)guanidino)phenyl)-1-(diphenoxy-phosphoryl)ethylcarbamate (12c). Compound **11c** was dissolved in 50% trifluoroacetic acid in CH_2Cl_2. After stirring for 3 h at room temperature, the solvent was evaporated. The crude oil was washed with cold ether and a precipitate was isolated. A mixture of the crude phosphonate (1 equiv), *N*,*N*′-

bis(*tert*-butyloxycarbonyl-1-guanyl-pyrazole (1 equiv), and triethylamine (3 equiv) in chloroform (20 mL) was stirred at room temperature for 3 days. The solvent was evaporated and the residue was dissolved in ethylacetate and washed with 1 N HCl, saturated solution of $NaHCO_3$ and brine. The organic layer was dried over Na_2SO_4. The solvent was evaporated and the crude product was purified by chromatography (0–80% EtOAc in hexane) to obtain the protected guanidine. Yield 62%; ^{1}H NMR ($CDCl_3$) δ 1.5 (d, 18H), 3.0–3.4 (m, 2H), 3.5 (s, 3H), 4.7 (m, 1H), 7.1–7.6 (m, 14H); HPLC (214 nm) t_r 17.2 min, 99.1%; HPLC (254 nm) t_r 17.2 min, 100.0%; LC/MS t_r 20.8 min, 98.9%; MS (ESI) m/z 691 $[M + Na]^+$.

Ethyl 2-(4-(*N*,*N*′-Bis(*tert*-butyloxycarbonyl)guanidino)phenyl)-1-(diphenoxy-phosphoryl)ethylcarbamate (12d). Same procedure as for **12c**. Yield 63%; ^{1}H NMR ($CDCl_3$) δ 1.3 (t, 3H), 1.5 (d, 18H), 3.0–3.4 (m, 2H), 4.0 (q, 2H), 4.7 (m, 1H), 5.6 (m, 1H), 7.1–7.6 (m, 14H); HPLC (214 nm) t_r 18.0 min, 97.4%; HPLC (254 nm) t_r 18.0 min, 100.0%; LC/MS t_r 20.9 min, 91.3%; MS (ESI) m/z 705 $[M + Na]^+$.

Methyl 1-(Bis(4-acetamidophenoxy)phosphoryl)-2-(4-(*tert*-butyloxycarbonylamino)phenyl)ethylcarbamate (Paracetamol Analogue of 11c). Acetamidophenyl phosphonates were prepared in the same way as the diphenyl phosphonates **11**, except tri-4-acetamidophenyl phosphite[16] was used instead of triphenyl phosphite, MeCN was used as solvent, and $TiCl_4$ as the catalyst. The product did not precipitate from MeOH and flash chromatography was necessary (EtOAC/MeOH) to isolate these compounds. Yield 39%; ^{1}H NMR ($CDCl_3$) δ 1.5 (s, 9H), 2.1 (2s, 6H), 2.8–3.3 (m, 2H), 3.3 (s, 3H), 4.5 (m, 1H), 6.8 (NH), 7.1–7.4 (m, 14H); MS (ESI) m/z 663 $[M + Na]^+$.

Methyl 1-(Bis(4-acetamidophenoxy)phosphoryl)-2-(4-(*N*,*N*′-bis(*tert*-butyloxycarbonyl)guanidino)phenyl)ethylcarbamate (Paracetamol Analogue of 12c). Same procedure as for **12c**. Yield 51%; ^{1}H NMR ($CDCl_3$) δ 1.5 (d, 18H), 2.1 (2s, 6H) 3.0–3.4 (m, 2H), 3.4 (s, 3H), 4.7 (m, 1H), 6.7 (m, 1H), 7.1–7.6 (m, 12H); MS (ESI) m/z 805 $[M + Na]^+$.

Diphenyl *N*-(Benzyloxycarbonylamino)-(3-guanidinopropyl)-methanephosphonate Trifluoroacetate (6a). The Boc-protected intermediate[10,16] was dissolved in 50% trifluoroacetic acid in CH_2Cl_2 (2–5 mL). After stirring for 3 h at room temperature, the solvent was evaporated. The crude oil was washed with cold ether and a precipitate was isolated. Yield 91%; ^{1}H NMR (CD_3OD, 400 MHz) δ 1.6 (m, 1H), 1.7–1.9 (m, 2H), 2.1 (m, 1H), 3.2 (m, 2H), 4.5 (m, 1H), 5.1 (q, 1H), 7.1–7.3 (m, 15H); HPLC (214 nm) t_r 19.1 min, 96.2%; HPLC (254 nm) t_r 19.0 min, 98.3%; LC/MS t_r 13.2 min, 100.0%; MS (ESI) m/z 497 $[M + H]^+$.

Diphenyl 1-(Benzyloxycarbonylamino)-2-(4-guanidinophenyl)-ethanephosphonate. Trifluoroacetate (6b). Same procedure as for **6a**. Yield 91%; ^{1}H NMR (CD_3OD, 400 MHz) δ 3.0 (m, 1H), 3.4 (m, 1H), 4.7 (m, 1H), 5.1 (m, 2H), 5.8 (s, 1H), 7.0–7.4 (m, 19H); HPLC (214 nm) t_r 21.1 min, 98.5%; HPLC (254 nm) t_r 21.0 min, 100.0%; LC/MS t_r 13.9 min, 100.0%; MS (ESI) m/z 545 $[M + H]^+$.

Methyl 1-(Diphenoxyphosphoryl)-2-(4-guanidinophenyl)ethylcarbamate Trifluoroacetate (6c). Same procedure as for **6a**. Yield 90%; ^{1}H NMR ($CDCl_3$) δ 2.9–3.4 (m, 2H), 4.5 (s, 3H), 4.7 (m, 1H), 7.0–7.5 (m, 14H); HPLC (214 nm) t_r 16.6 min, 100.0%; HPLC (254 nm) t_r 16.6 min, 100.0%; LC/MS t_r 11.2 min, 100.0%; MS (ESI) m/z 469 $[M + H]^+$.

Ethyl 1-(Diphenoxyphosphoryl)-2-(4-guanidinophenyl)ethylcarbamate Trifluoroacetate (6d). Same procedure as for **6a**. Yield 89%; ^{1}H NMR ($CDCl_3$) δ 1.2 (t, 3H), 3.0–3.4 (m, 2H), 4.3 (q, 2H), 4.7 (m, 1H), 7.0–7.5 (m, 14H); HPLC (214 nm) t_r 16.7 min, 100.0%; HPLC (254 nm) t_r 16.7 min, 100.0%; LC/MS t_r 11.5 min, 100.0%; MS (ESI) m/z 483 $[M + H]^+$.

Diphenyl 1-Amino-2-(4-guanidinophenyl)ethylphosphonate 2 Trifluoroacetate (6k). Intermediate **13**[10,16] was dissolved in 50% trifluoroacetic acid in CH_2Cl_2 (2–5 mL). After stirring for 3 h at room temperature, the solvent was evaporated. The crude oil was washed with cold ether and a precipitate was isolated. Yield 83%; ^{1}H NMR ($CDCl_3$) δ 3.0–3.4 (m, 2H), 4.7 (m, 1H), 7.0–7.4 (m, 14H). HPLC (214 nm) t_r 7.2 min, 91.5%; HPLC (254 nm) t_r 7.1 min, 95.1%; LC/MS t_r 10.3 min, 93.1%; MS (ESI) m/z 411 $[M + H]^+$.

Acetylation or Sulfonylation of Compound 13 and Deprotection of Intermediates Leading to Compounds 6e−j and 8c. A suspension of **13**[10,16] and triethylamine in dichloromethane was cooled at −30 °C, and the corresponding acetyl chloride or sulfonylchloride in dichloromethane was added dropwise. After 10 min, the reaction was quenched by adding 1 mL of water and the organic layer was washed with saturated sodium bicarbonate solution. After drying on sodium sulfate, the solvent was evaporated and the product was purified by chromatography; ethyl acetate/hexane (0→80%).

The intermediate was dissolved in 50% trifluoroacetic acid in CH_2Cl_2 (2–5 mL). After stirring for 3 h at room temperature, the solvent was evaporated. The crude oil was washed with cold ether and a precipitate was isolated.

Diphenyl 1-Acetamido-2-(4-guanidinophenyl)ethylphosphonate Trifluoroacetate (6e). Intermediate diphenyl 1-acetamido-2-(4-(*N*,*N*′-bis(*tert*-butyloxycarbonyl)guanidino)phenyl)-ethylphosphonate. ^{1}H NMR ($CDCl_3$) δ 1.5 (d, 18H), 1.7 (s, 3H), 3.0–3.4 (m, 2H), 5.1 (m, 1H), 5.9 (NH), 7.1–7.6 (m, 14H), 10.3 (NH), 11.6 (NH); HPLC (214 nm) t_r 26.7 min, 100%; HPLC (254 nm) t_r 26.7 min, 100%; LC/MS t_r 20.5 min, 100.0%; MS (ESI) m/z 675 $[M + Na]^+$. **6e**: Yield 96%; ^{1}H NMR ($CDCl_3$) δ 1.7 (s, 3H), 3.0–3.4 (m, 2H), 5.0 (m, 1H), 6.5 (NH), 7.0–7.5 (m, 14H), 10.0 (NH); HPLC (214 nm) t_r 15.3 min, 100%; HPLC (254 nm) t_r 15.3 min, 100.0%; LC/MS t_r 12.2 min, 100.0%; MS (ESI) m/z 453 $[M + H]^+$.

Diphenyl 1-(Benzoylamino)-2-(4-guanidinophenyl)-ethanephosphonate Trifluoroacetate (6f). Intermediate (diphenyl 1-(benzoylamino)-2-{4-[*N*,*N*′-bis(*tert*-butyloxycarbonyl)guanidine]phenyl}ethanephosphonate. Yield 10%; ^{1}H NMR ($CDCl_3$, 400 MHz) δ 1.5 (18H, d), 3.2 (m, 1H), 3.4 (m, 1H), 3.4 (m, 1H), 5.4, (m, 1H), 7.1–7.5 (m, 19H), 7.6 (d, 2H), 10.3 (s, 1H), 11.5 (s, 1H); MS (ESI) m/z 715 $[M + H]^+$. **6f**: Yield 80%; ^{1}H NMR (CD_3OD, 400 MHz) δ 3.2 (m, 1H), 3.4 (m, 1H), 4.7 (m, 1H), 6.6 (m, 2H), 7.1 (m, 5H), 7.3–7.5 (m, 8H), 7.6 (m, 3H), 8.0 (d, 1H); HPLC (214 nm) t_r 20.0 min, 100.0%; HPLC (254 nm) t_r 21.0 min, 100.0%; LC/MS t_r 13.3 min, 91.2%; MS (ESI) m/z 515 $[M + H]^+$.

Diphenyl 1-(*o*-Toluenesulfonylamino)-2-(4-guanidinophenyl)-ethanephosphonate Trifluoroacetate (6g). Intermediate diphenyl 1-(α-toluenesulfonylamino)-2-{4-[*N*,*N*′-bis(tert-butyloxycarbonyl)guanidine]phenyl} ethanephosphonate. Yield 32%; ^{1}H NMR ($CDCl_3$, 400 MHz) δ 1.5 (18H, d), 3.1 (m, 2H), 3.4 (m, 1H), 3.8 (d, 1H), 4.0 (d, 1H), 4.6 (m, 1H), 5.1 (d, 1H), 7.1–7.3 (m, 17H), 7.6 (d, 2H), 10.3 (s, 1H), 11.5 (s, 1H). **6g**: Yield 94%; ^{1}H NMR (CD_3OD, 400 MHz) δ 3.1 (m, 1H), 3.5 (m, 1H), 4.1 (d, 1H), 4.2 (d, 1H), 4.6 (m, 1H), 7.2–7.5 (m, 19H); HPLC (214 nm) t_r 20.2 min, 94.1%; HPLC (254 nm) t_r 20.2 min, 100.0%; LC/MS t_r 14.0 min, 100.0%; MS (ESI) m/z 565 $[M + H]^+$.

Diphenyl 1-(Naphthalenesulfonylamino)-2-(4-guanidinophenyl)-ethanephosphonate Trifluoroacetate (6h). Intermediate diphenyl 1-(*N*-naphthalenesulfonylamino)-2-{4-[*N*,*N*′-bis(*tert*-butyloxycarbonyl)guanidine]phenyl}ethanephosphonate. Yield 23%; ^{1}H NMR ($CDCl_3$, 400 MHz) δ 1.6 (18H, d), 3.0–3.2 (m, 2H), 4.5 (m, 1H), 6.0 (d, 1H), 6.6 (d, 2H), 6.9–7.6 (15H), 7.8 (d, 1H), 7.9 (d, 1H), 8.1 (d, 1H), 8.5 (d, 1H), 10.0 (s, 1H), 11.6 (s, 1H). **6h**: Yield 93%; ^{1}H NMR ($CDCl_3$, 400 MHz) δ 3.0 (m, 1H), 3.4 (m, 1H), 4.4 (m, 1H), 6.7 (d, 2H), 6.9 (d, 4H), 7.1–7.4 (11H), 7.6 (t, 1H), 7.7 (t, 1H) 7.9 (m, 1H), 8.1 (d, 1H); HPLC (214 nm) t_r 20.6 min, 96.3%; HPLC (254 nm) t_r 21.0 min, 100.0%; LC/MS t_r 14.7 min, 100.0%; MS (ESI) m/z 601 $[M + H]^+$.

Diphenyl 1-(2,3,6-Tri-isopropylbenzenesulfonyl)amino-2-(4-guanidinophenyl)-ethanephosphonate Trifluoroacetate (6i). Intermediate diphenyl 1-(*N*-2,3,6-tri-isopropylbenzenesulfonylamino)-2-{4-[*N*,*N*′-bis(*tert*-butyloxycarbonyl)guanidine]phenyl} ethanephosphonate. Yield 14%; ^{1}H NMR ($CDCl_3$, 400 MHz) δ 1.2–1.4 (m, 18H), 1.5 (d, 18H), 2.9–3.0 (m, 1H), 3.3–3.5 (m, 2H), 4.1 (m, 1H), 4.2 (m, 1H), 4.4 (m, 1H), 5.0 (d, 1H), 6.7 (d, 2H), 6.9 (d, 2H), 7.1–7.3 (m, 8H), 7.4 (d, 2H), 7.5 (d, 2H). **6i**: Yield 89%; ^{1}H NMR (CD_3OD, 400 MHz) δ 1.2–1.4 (m, 18H), 2.3 (m, 1H), 3.0–3.1 (m, 2H),

4.1–4.3 (3H), 7.0–7.6 (m, 16H); HPLC (214 nm) t_r 26.9 min, 100.0%; HPLC (254 nm) t_r 26.9 min, 100.0%; LC/MS t_r 18.0 min, 99.0%; MS (ESI) m/z 677 $[M + H]^+$.

Diphenyl 1-(Methylsulfonylamino)-2-(4-guanidinophenyl)-ethanephosphonate Trifluoroacetate (6j). Intermediate diphenyl 1-(methylsufonylamino)-2-{4-[*N*,*N*′-bis(*tert*-butyloxycarbonyl)guanidine]phenyl}ethanephosphonate. Yield 18%; ^{1}H NMR ($CDCl_3$, 400 MHz) δ 1.5 (d, 18H), 2.5 (s, 3H), 3.0 (m, 1H), 3.5 (m, 1H), 4.5 (m, 1H), 5.6 (d, 1H), 7.1–7.6 (m, 14), 10.3 (s, 1H), 11.6 (s, 1H). **6j**: Yield 92%; ^{1}H NMR (CD_3OD, 400 MHz) δ 3.1 (m, 1H), 3.5 (m, 1H), 4.5 (m, 1H), 7.2 (m, 8H), 7.4 (m, 4H), 7.45 (d, 2H); HPLC (214 nm) t_r 18.2 min, 98.0%; HPLC (254 nm) t_r 17.3 min, 100.0%; LC/MS t_r 12.8 min, 96.3%; MS (ESI) m/z 489 $[M + H]^+$.

Diphenyl 1-(*N*-Benzyloxycarbonylamino)-1-(4-amidinophenyl)methanephosphonate·HCl (7a). Compound was synthesized as repoterted by Oleksyszyn et al.[12] ^{1}H NMR (CD_3OD, 400 MHz) δ 2.0 (3H, s), 5.1 (q, 2H), 7.0 (m, 4H), 7.2–7.4 (m, 11H), 7.8 (s, 4H), HPLC (214 nm) t_r 20.6 min, 100.0%; HPLC (254 nm) t_r 20.5 min, 100.0%; LC/MS t_r 13.9 min, 98.4%; MS (ESI) m/z 516 $[M + H]^+$.

Diphenyl 1-(*N*-Benzyloxycarbonylamino)-2-(4-amidinophenyl) Ethanephosphonate·HCl (7b). Compound was synthesized as reported by Oleksyszyn et al.[12] ^{1}H NMR (CD_3OD, 400 MHz) δ 2.0 (4H, s), 3.1 (m, 1H), 3.5 (m, 1H), 4.7 (m, 1H), 5.0 (q, 2H), 7.1–7.4 (m, 15H), 7.5 (d, 2H), 7.7 (d, 2H); HPLC (214 nm) t_r 20.2 min, 90.3%; HPLC (254 nm) t_r 20.2 min, 91.3%; LC/MS t_r 13.6 min, 92.2%; MS (ESI) m/z 530 $[M + H]^+$.

Diphenyl 1-(*N*-Benzyloxycarbonylamino)-1-(4-amidinophenyl)propanephosphonate·HCl (7c). 4-Cyanobenzaldehyde (**15a**; 5 g, 0.038 mol) and triphenylphosphoranylidene acetic acid ethyl ester (16 g, 0.045 mol) were dissolved in dry toluene (70 mL), and the solution was stirred at room temperature for 12 h. Then the solvent was removed under vacuum, and the residue was taken up with ether. The solid formed was removed by filtration and the organic phase was evaporated to give 3-(4-cyano-phenyl)-3-propenoic acid ethyl ester as yellow oil. The compound was purified with flash chromatography (hex/EtOAc). After evaporation of the desired fractions, a white semi solid was obtained (6 g). The product was dissolved in ethanol and added dropwise to a suspension of sodium borohydride (11 g, 0.28 mol) in ethanol (100 mL) cooled at 0 °C. The mixture was allowed to reach room temperature, and stirring was maintained for 18 h. Acetone (5 mL) in 20 mL of water was added dropwise to the mixture to destroy the remaining $NaBH_4$. The solvent was evaporated and water was added. This solution was three times extracted with EtOAc. The combined organic solutions were washed twice with 2 N HCl and once with brine. The organic phase was dried and subsequent to evaporation of the solvent a light yellow oil was obtained (3g, 47% yield). 3-(4-Cyanophenyl)propanol was oxidized with the Dess-Martin reagent to the aldehyde (**15c**). The crude product was immediately dissolved in CH_2Cl_2 without any further purification. The same procedure as for **11b** was used to prepare the diphenyl phosphonate **16c**. The obtained product was purified with flash chromatography, 21% yield starting from 3-(4-cyanophenyl)propanol. ^{1}H NMR ($CDCl_3$, 400 MHz) δ 2.1 (m, 1H), 2.35 (m, 1H), 2.8 (m, 1H), 2.9 (m, 1H), 4.5 (m, 1H), 5.1 (m, 2H), 5.7 (d, 1H), 7.1–7.4 (m, 16H), 7.5 (m, 3H); MS (ESI) m/z 527 $[M + H]^+$.

Diphenyl 1-(*N*-(benzyloxycarbonyl)amino-1-(4 cyanophenyl-)propanephosphonate was dissolved in dry chloroform/methanol (1:1). The mixture was cooled to 0 °C and saturated with dry HCl gas. The mixture was stirred for 3 days at 0 °C. The solvent was evaporated, and the crude product was precipitated from dry ether. The product was dissolved in 4 equiv of a 2 M solution of ammonia in ethanol. The solution was stirred for 2 days at room temperature. The solvent was evaporated. The product was washed with EtOAc saturated with HCl. The product was precipitated from diethyl ether. Yield 15%; ^{1}H NMR (CD_3OD, 400 MHz) δ 2.2 (m, 1H), 2.35 (m, 1H), 2.8 (m, 1H), 3.05 (m, 1H), 4.3 (m, 1H), 5.1 (q, 2H), 7.1–7.4 (m, 17H), 7.7 (d, 2H); HPLC (214 nm) t_r 20.6 min, 92.0%; HPLC (254 nm) t_r 20.6 min, 93.0%; LC/MS t_r 14.7 min, 97.0%; MS (ESI) m/z 544 $[M + H]^+$.

Di-(4-acetamidophenyl) 1-(benzyloxycarbonylamino)-2-[(4-guanidino)phenyl]ethanephosphonate Trifluoroacetate (8a). Same procedure as for **6a**. Yield 95%; ^{1}H NMR (CD_3OD, 400 MHz) δ 2.0 (s, 6H), 3.0 (m, 1H), 3.4 (m, 1H), 4.6 (m, 1H), 5.1 (m, 2H), 6.7–7.3 (m, 17H), 8.0 (d, 1H); HPLC (214 nm) t_r 15.7 min, 95.0%; HPLC (254 nm) t_r 15.7 min, 94.2%; LC/MS t_r 12.1 min, 95.3%; MS (ESI) m/z 659 $[M + H]^+$.

Methyl 1-(Bis(4-acetamidophenoxy)phosphoryl)-2-(4guanidino-phenyl)ethylcarbamate Trifluoroacetate (8b). Same procedure as for **6a**. Yield 94%; ^{1}H NMR ($CDCl_3$) δ 2.1 (2s, 6H), 2.9–3.4 (m, 2H), 4.6 (s, 3H), 4.7 (m, 1H), 7.0–7.5 (m, 12H); HPLC (214 nm) t_r 10.9 min, 98.0%; LC/MS t_r 10.7 min, 96.4%; MS (ESI) m/z 583 $[M + H]^+$.

Di-(4-acetamidophenyl) 1-(methylsulfonylamino)-2-(4-guanidinophenyl)-ethanephosphonate Trifluoroacetate (8c). Intermediate di-(4-acetamidophenyl) 1-(methylsufonylamino)-2-{4-[*N*,*N*′-bis(*tert*-butyloxycarbonyl)guanidino]phenyl} ethanephosphonate. Yield 18%; ^{1}H NMR ($CDCl_3$, 400 MHz) δ 1.5 (d, 18H), 2.0 (s, 3H), 2.1 (s, 3H), 2.2 (s, 3H), 2.9 (m, 1H), 3.3 (m, 1H), 4.3 (m, 1H), 7.1–7.6 (m, 12), 8.3 (s, 1H), 8.6 (s, 1H), 10.3 (s, 1H), 11.6 (s, 1H); MS (ESI) m/z 803 $[M + H]^+$. **8c**: Yield 91%; ^{1}H NMR (CD_3OD, 400 MHz) δ 2.1 (s, 6H), 2.7 (s, 3H), 3.1 (m, 1H), 3.5 (m, 1H), 4.5 (m, 1H), 7.1 (m, 4H), 7.2 (d, 2H), 7.45 (d, 2H), 7.6 (d, 4H); HPLC (214 nm) t_r 12.2 min, 93.2%; HPLC (254 nm) t_r 11.6 min, 94.1%; LC/MS t_r 10.7 min, 100.0%; MS (ESI) m/z 603 $[M + H]^+$.

uPA Inhibition: In Vitro Evaluation. Enzymatic activity was measured at 37 °C in a Spectramax 340 (Molecular Devices) microtiter plate reader using the chromogenic substrate S-2444 (LpyroGlu-Gly L-Arg-*p*-NA·HCl), with a K_m of 80 μM. The substrate was obtained from Chromogenix. The human enzyme was obtained from Sigma-Aldrich and the mouse uPA was obtained from Molecular Innovations, Inc. (U.S.A.). The reaction was monitored at 405 nm, and the initial rate was determined between 0 and 0.25 absorbance units in 20 min. The reaction mixture contained 250 μM substrate and approximately 1 mU of enzyme in 145 μL of buffer in a final volume of 200 μL. A 50 mM Tris buffer, pH 8.8, was used. From each inhibitor concentration, 5 μL was added, obtaining a final concentration from 0 to 250 μM in a total volume of 0.2 mL. Activity measurements were routinely performed in duplicate. The IC_{50} value is defined as the concentration of inhibitor required to reduce the enzyme activity to 50% after a 15 min preincubation with the enzyme at 37 °C before addition of the substrate. IC_{50} values were obtained by fitting the data with the four-parameter logistics equation using Grafit 5.

$$v = (v \text{ range})/(1 + \exp(s \times \ln(\text{abs}(I_0/IC_{50})) + \text{background}$$

where s = slope factor, v = rate, I_0 = inhibitor concentration, and range = the fitted uninhibited value minus the background. The equation assumes the y falls with increasing x.

Inhibitor stock solutions were prepared in DMSO and stored at −20 °C. Because the compounds described in this paper completely inactivate uPA following pseudofirst-order kinetics, the IC_{50} value is inversely correlated with the second-order rate constant of inactivation. For a simple pseudofirst-order inactivation process, the activity after incubation with inhibitor (v_i) varies with the inhibitor concentration (i), as described in the following equation: $v_i = v_0 \times e^{-k_i t}$, where v_0 is the activity in absence of inhibitor, k is the second-order rate constant of inactivation, and t is the time. The inactivation rate constant was determined from the time course of inhibition.

The inhibitor was mixed with the substrate (250 μM final concentration), and the buffer solution with the enzyme was added at the time zero. The inhibitor concentrations were chosen to obtain total inhibition of the enzyme within 20 min. The progress curves show the absorbance of *p*-nitroanilide produced as a function of time. Initially, no inhibitor is bound to the enzyme, and the tangent to the progress curve (dA/dt) is proportional to the concentration of the free enzyme. The concentration of free enzyme decreases over time due to the kinetics of inhibitor binding, as described

above. Progress curves were recorded in pseudofirst-order conditions ($[I]_0 >> [E]_0$) and with less than 10% conversion of the substrate during the entire time course. In these conditions, dA/dt decreases exponentially with time. The progress curves were fitted with the integrated rate equation to yield a value for k_{obs}, a pseudofirst-order rate constant

$$A_t = v_0[1 - \exp(-k_{obs}t)]/k_{obs} + A_0 \quad (1)$$

where A_t = absorbance at time t, A_0 = absorbance at time zero, and v_0 = uninhibited initial rate. The apparent second-order rate constant (k_{app}) was calculated from the slope of the linear part of the plot of k_{obs} versus the inhibitor concentration ($[I]_0$). In case of competition between the inhibitor and the substrate, k_{app} is smaller than the "real" second order rate constant k discussed above because a certain fraction of the enzyme is present as an enzyme–substrate complex. k_{app} depends on the substrate concentration used in the experiment, as described by Lambeir et al.[26]

For inhibitors **6a**, **6c**, **6d**, **6f**, **7b**, and **8a**, the k_{obs} versus $[I]_0$ plot was not linear, but could be fitted with a hyperbolic function: $k_{obs} = k_2[I]_0/(K_1 + [I]_0)$ (two step mechanism).

Where K_1 is the dissociation constant of the reversible enzyme–inhibitor complex and k_2 is the first-order rate constant associated with irreversible modification of the enzyme. A k_{app} could be calculated as k_2/K_1.

Determination of the Selectivity for uPA. The IC_{50} values for plasmin (from human plasma, Sigma), tPA (recombinant, Boehringer Ingelheim), thrombin (from human plasma, Sigma), and FXa were determined in the same way as for uPA. S-2288 (H-D-Ile-Pro-Arg-pNa·2HCl) for tPA (K_m: 1 mM), S-2366 (pyroGlu-Pro-Arg-pNA·HCl) for plasmin (K_m: 400 μM) and thrombin (K_m: 150 μM), and S-2772 (Boc-D-Arg-Gly ArgpNA·2HCl) for FXa (K_m: 1.5 mM) were used as substrates. FX (Sigma) is activated with Russel's viper venom (Sigma). The mixture contained 580 μM substrate for thrombin and plasmin, 1.25 mM for tPA, 522 μM for FXa, and 425 μM for trypsin, approximately 5 mU of enzyme, and 145 μL of buffer. For tPA and thrombin, Tris buffer, pH 8.3, was used, for FXa, Tris buffer, pH 8.3, with 2.5 mM $CaCl_2$ was used, for plasmin, Tris buffer, pH 7.4, was used. The selectivity index was calculated as (IC_{50} enzyme X)/IC_{50} uPA, where X is tPA, thrombin, plasmin or FXa.

Molecular Modeling. The molecular modeling studies were performed using MOE 2006.08 software (Chemical Computing Group). All software necessary to build compounds and perform minimizations, alignment, and superposition is available in the MOE package and was used with standard settings, unless otherwise mentioned. Crystal structures were downloaded from the Protein Databank (PDB) and the ligands were checked and corrected when necessary. Residues not belonging to the enzyme or ligand were removed, including water molecules. Hydrogen atoms were added and energy minimized with MMFF94x force field (standard parameters) keeping all heavy atoms fixed.

Following PDB structures of uPA were used: 1EJN,[25] 1F5K,[27] 1F5L,[27] 1F92,[27] 1FV9,[28] 1LMW,[29] 1SC8,[4] 1VJ9,[4] 1VJA.[4]

All structures were aligned and superposed. The studied compounds were built using different parts of these ligands in the mentioned enzymes followed by covalent linkage to the side chain oxygen of Ser195. Then the complex was minimized using MMFF94x force field with a flexible ligand in a rigid enzyme. Ser 195 residue of 1EJN was kept flexible during simulations. The following PDB files were used to study the selectivity toward related enzymes: tPA (1A5H,[30] 1RTF[31]), thrombin (1DWB,[32] 1GJ4,[33] 1H8I[34]), plasmin (1BUI[35]), FXa (1FAX,[36] 1KYE,[37] 1MQ6[38]), trypsin (1H4W,[39] 1EB2,[40] 1MAX[41]).

Evaluation of the Stability, logD, and Apparent Solubility. Chemical Stability. The chemical stability was measured at buffer pH of 1, 4, 7.4, and 8.8 at 37 °C. Stock solutions of 8 mg/mL of **6c** and 4 mg/mL of **8b** in MeOH were prepared. Each stock solution was divided in 4 fractions of 250 μL each. These fractions were diluted with the buffers solution to obtain approximately 0.3 g/mL in each buffer solution. Samples are taken at time 0, 1 h 30 min, 3 h, 6 h, 12 h, 24 h, 48 h, 1 week, and 2 weeks. The samples (100 μL) were not diluted and were immediately analyzed by HPLC (214 nm). The evolution of the AUC (area under the curve) of the parent compound in function of time was taken as a parameter for chemical stability. The following buffers were used: 125 mM aqueous HCl, pH 1.1; 100 mM HOAc, 18 mM NaOAc, pH 4; 50 mM Tris, pH 7.4, 110 mM NaCl, and 50 mM Tris, pH 8.8, 38 mM NaCl. The amount corresponding to the indicated molarity was weighed/measured and dissolved/diluted in water, and the pH was adjusted with diluted solutions of HCl or ammonium hydroxide, depending on the required pH.

Log D. A total of 40 μL of a 10 mM stock solution in DMSO was added to 1.960 mL of a mixture of octanol and phosphate buffer saline (PBS), pH 7.4 (1/1). Octanol was first saturated with PBS and PBS was first saturated with octanol before the two solvents were mixed. After two hours of shaking at room temperature, the two layers were separated. A total of 10 μL of each layer was added to 390 μL of MeOH before the sample was analyzed with LC/MS/MS. The logD is calculated from the formula: $\text{LogD} = \log(\text{AUC}_{\text{octanol}}/\text{AUC}_{\text{PBS}})$. The experiment was done in duplicate.[42]

Apparent Solubility. A total of eight different dilutions of an initial 10 mM test compound solution were prepared in DMSO. Each dilution was further diluted in PBS pH 7.4 to give a final DMSO concentration of 2% and final test compound concentration range of between 1 μM and 200 μM (4 μL DMSO solution in 196 μL buffer solution). Two replicates were prepared per concentration in a 96 well microtiter plate. The plates were incubated for 2 h at 37 °C. Absorbance was measured at 620 nm and solubility was determined by an increase in absorbance.

Plasma Stability. A 40 μL aliquot of the 10 mM solution in DMSO of the test compound was added to 1.990 mL of human plasma to obtain a 200 μM final solution. The mixture was gently shaken for 24 h at 37 °C. Aliquots of 200 μL were taken at various time points (0, 30 min, 1 h, 2 h, 3 h, 6 h, and 24 h) and diluted with 400 μL of methanol. The suspension was centrifuged at 14000 rpm for 5 min at 4 °C. A total of 10 μL of the supernatant was diluted with 990 μL of a 0.2 μM solution of the standard UMAC00150 in MeOH and analyzed with LC/MS/MS. The samples were analyzed in triplicate.

Acknowledgment. This work received support from the Fund for Scientific Research-Flanders (Belgium; FWO). P.V.d.V. is a postdoctoral fellow of the FWO and G.S. is a visiting postdoctoral fellow of the FWO. J.J. was a fellow of the Institute of Promotion of Innovation in Science and Technology of Flanders (IWT). Currently J.J. is coordinator of the Antwerp Drug Discovery Network (ADDN) financed by the Industrial Development Fund (IOF) of the University of Antwerp. The excellent technical assistance of W. Bollaert is greatly appreciated.

Supporting Information Available: The experimental details for the intermediates **10**, **11b**, **12b**, **13**, and tri-4-acetamidophenyl phosphite and a purity table for all end compounds. Extra enzyme kinetic data for the compounds **6a**, **6c**, **6f**, **7b**, and **8a**, as well as plasma stability of compounds **6c** and **8b**. Also the complete experimental details for the BN-472 rat mammary carcinoma model is available. This material is available free of charge via the Internet at http://pubs.acs.org.

References

(1) Dano, K.; Behrendt, N.; Hoyer-Hansen, G.; Johnsen, M.; Lund, L. R.; Ploug, M.; Romer, J. Plasminogen Activation and Cancer. *Thromb. Haemostasis* **2005**, *93*, 676–681.

(2) Mazzieri, R.; Blasi, F. The Urokinase Receptor and the Regulation of Cell Proliferation. *Thromb. Haemostasis* **2005**, *93*, 641–646.

(3) Duffy, M. J. The Urokinase Plasminogen Activator System: Role in Malignancy. *Curr. Pharm. Des.* **2004**, *10*, 39–49.

(4) Schweinitz, A.; Steinmetzer, T.; Banke, I. J.; Arlt, M. J. E.; Sturzebecher, A.; Schuster, O.; Geissler, A.; Giersiefen, H.; Zeslawska, E.; Jacob, U.; Kruger, A.; Sturzebecher, J. Design of Novel and Selective Inhibitors of Urokinase-Type Plasminogen Activator With

Improved Pharmacokinetic Properties for Use As Antimetastatic Agents. *J. Biol. Chem.* **2004**, *279*, 33613–33622.

(5) Setyono-Han, B.; Sturzebecher, J.; Schmalix, W. A.; Muehlenweg, B.; Sieuwerts, A. M.; Timmermans, M.; Magdolen, V.; Schmitt, M.; Klijn, J. G. M.; Foekens, J. A. Suppression of Rat Breast Cancer Metastasis and Reduction of Primary Tumour Growth by the Small Synthetic Urokinase Inhibitor WX-UKI. *Thromb. Haemostasis* **2005**, *93*, 779–786.

(6) www.wilex.com, accessed June, 2007.

(7) Rockway, T. W.; and Giranda, V. L. Inhibitors of the Proteolytic Activity of Urokinase Type Plasminogen Activator. *Curr. Pharm. Des.* **2003**, *9*, 1483–1498.

(8) Ke, S.-H.; Coombs, G. S.; Tachias, K.; Corey, D. R.; Madison, E. L. Optimal Subsite Occupancy and Design of a Selective Inhibitor of Urokinase. *J. Biol. Chem.* **1997**, *272*, 20456–20462.

(9) Mackman, R. L.; Katz, B. A.; Breitenbucher, J. G.; Hui, H. C.; Verner, E.; Luong, C.; Liu, L.; Sprengeler, P. A. Exploiting Subsite S1 of Trypsin-Like Serine Proteases for Selectivity: Potent and Selective Inhibitors of Urokinase-Type Plasminogen Activator. *J. Med. Chem.* **2001**, *44*, 3856–3871.

(10) Joossens, J.; Van der Veken, P.; Lambeir, A. M.; Augustyns, K.; Haemers, A. Development of Irreversible Diphenyl Phosphonate Inhibitors for Urokinase Plasminogen Activator. *J. Med. Chem.* **2004**, *47*, 2411–2413.

(11) Tamura, S. Y.; Weinhouse, M. I.; Roberts, C. A.; Goldman, E. A.; Masukawa, K.; Anderson, S. M.; Cohen, C. R.; Bradbury, A. E.; Bernardino, V. T.; Dixon, S. A.; Ma, M. G.; Nolan, T. G.; Brunck, T. K. Synthesis and Biological Activity of Peptidyl Aldehyde Urokinase Inhibitors. *Bioorg. Med. Chem. Lett.* **2000**, *10*, 983–987.

(12) Oleksyszyn, J.; Boduszek, B.; Kam, C. M.; Powers, J. C. Novel Amidine-Containing Peptidyl Phosphonates As Irreversible Inhibitors for Blood-Coagulation and Related Serine Proteases. *J. Med. Chem.* **1994**, *37*, 226–231.

(13) Belyaev, A.; Zhang, X. M.; Augustyns, K.; Lambeir, A. M.; De Meester, I.; Vedernikova, I.; Scharpe, S.; Haemers, A. Structure−Activity Relationship of Diaryl Phosphonate Esters As Potent Irreversible Dipeptidyl Peptidase IV Inhibitors. *J. Med. Chem.* **1999**, *42*, 1041–1052.

(14) Peterlin-Masic, L.; Kikelj, D. *Arginine mimetics. Tetrahedron* **2001**, *57*, 7073–7105.

(15) Zeslawska, E.; Jacob, U.; Schweinitz, A.; Coombs, G.; Bode, W.; Madison, E. Crystals of Urokinase Type Plasminogen Activator Complexes Reveal the Binding Mode of Peptidomimetic Inhibitors. *J. Mol. Biol.* **2003**, *328*, 109–118.

(16) Joossens, J.; Van der Veken, P.; Surpateanu, G.; Lambeir, A.-M.; El-Sayed, I.; Ali, O. M.; Augustyns, K.; Haemers, A. Diphenyl Phosphonate Inhibitors for the Urokinase-Type Plasminogen Activator: Optimization of the P4 Position. *J. Med. Chem.* **2006**, *49*, 5785–5793.

(17) University of Antwerp, Novel Urokinase Inhibitors, WO2007045496, 2007.

(18) Sienczyk, M.; Oleksyszyn, J. Inhibition of Trypsin and Urokinase by Cbz-amino(4-guanidino-phenyl)methanephosphonate Aromatic Ester Derivatives: The Influence of the Ester Group on their Biological Activity. *Bioorg. Med. Chem. Lett.* **2006**, *16*, 2886–2890.

(19) Grzywa, R.; Dyguda-Kazimierowicz, E.; Sienczyk, M.; Feliks, M.; Sokalski, A. W.; Oleksyszyn, J. The Molecular Basis of Urokinase Inhibition: From the Nonemperical Analysis of Intermolecular Interactions to the Prediction of Binding Affinity. *J. Mol. Model.* **2007**, *13*, 677–683.

(20) Dess, D. B.; Martin, J. C. *J. Org. Chem.* **1983**, *48*, 4156–4158.

(21) Van der Veken, P.; El Sayed, I.; Joossens, J.; Stevens, C. V.; Augustyns, K.; Haemers, A. Lewis Acid-Catalyzed Synthesis of *N*-Protected Diphenyl 1-Aminoalkylphosphonates. *Synthesis* **2005**, 634–638.

(22) Jackson, S. D.; Fraser, S. A.; Ni, L.-M.; Kam, C.-M.; Winkler, U.; Johnson, D. A.; Froelich, C. J.; Hudig, D.; Powers, J. C. Synthesis and Evaluation of Diphenyl Phosphonate Esters as Inhibitors of the Trypsin-Like Granzymes A and K and Mast Cell Tryptase. *J. Med. Chem.* **1988**, *41*, 2289–2301.

(23) Baraldi, G. P.; Cacciari, B.; Romagnoli, R.; Spalluto, G.; Monopoli, A.; Ongini, E.; Varani, K.; Borea, P. A. 7-Substituted 5-Amino-2-(2-furyl)pyrazolo[4,3-*e*]-1,2,4-triazolo[1,5-*c*]pyrimidines as A_{2A} Adenosine Receptor Antagonists: A Study on the Importance of Modifications at the Side Chain on the Activity and Solubility. *J. Med. Chem.* **2002**, *45*, 115–126.

(24) Wilex, Selective Urokinase Inhibitors, US20040266766, 2004.

(25) Sperl, S.; Jacob, U.; de Prada, N. A.; Sturzebecher, J.; Wilhelm, O. G.; Bode, W.; Magdolen, V.; Huber, R.; Moroder, L. (4-Aminomethyl) Phenylguanidine Derivatives as Nonpeptidic Highly Selective Inhibitors of Human Urokinase. *Proc. Natl. Acad. Sci. U.S.A.* **2000**, *97*, 5113–5118.

(26) Lambeir, A. M.; Borloo, M.; DeMeester, I.; Belyaev, A.; Augustyns, K.; Hendriks, D.; Scharpe, S.; Haemers, A. Dipeptide-Derived Diphenyl Phosphonate Esters: Mechanism-Based Inhibitors of Dipeptidyl Peptidase IV. *Biochim. Biophys. Acta* **1996**, *1290*, 76–82.

(27) Zeslawska, E.; Schweinitz, A.; Karcher, A.; Sondermann, P.; Sperl, S.; Sturzebecher, J.; Jacob, U. Crystals of the Urokinase-Type Plasminogen Activator Variant β(c)-uPAin Complex with Small Molecule Inhibitors Open the Way Towards Structure-Based Drug Design. *J. Mol. Biol.* **2000**, *11*, 465–475.

(28) Hajduk, P. J.; Boyd, S.; Nettesheim, D.; Nienaber, V.; Severin, J.; Smith, R.; Davidson, D.; Rockway, T.; Fesik, S. W. Identification of Novel Inhibitors of Urokinase via NMR-Based Screening. *J. Med. Chem.* **2000**, *43*, 3862–3866.

(29) Spraggon, G.; Phillips, C.; Nowak, U. K.; Ponting, C. P.; Saunders, D.; Dobson, C. M.; Stuart, D. I.; Jones, E. Y. The Crystal Structure of the Catalytic Domain of Human Urokinase-Type Plasminogen-Activator. *Structure* **1995**, *3*, 681–691.

(30) Renatus, M.; Bode, W.; Huber, R.; Sturzebecher, J.; Prasa, D.; Fischer, S.; Kohnert, U.; Stubbs, M. T. Structural Mapping of the Active Site Specificity Determinants of Human Tissue-Type Plasminogen Activator. Implications for the Design of Low Molecular Weight Substrates and Inhibitors. *J. Biol. Chem.* **1997**, *272*, 21713–21714.

(31) Lamba, D.; Bauer, M.; Huber, R.; Fischer, S.; Rudolph, R.; Kohnert, U.; Bode, W. The 2.3 Å Crystal Structure of the Catalytic Domain of Recombinant Two-Chain Human Tissue-Type plasminogen Activator. *J. Mol. Biol.* **1996**, *258*, 117–135.

(32) Banner, D. W. Hadvary, P. Crystallographic Analysis at 3.0-A Resolution of the Binding to Human Thrombin of Four Active Site-Directed Inhibitors. *J. Biol. Chem.* **1991**, *266*, 20085–20093.

(33) Griffith, S. C.; Sawaya, M. R.; Boutz, D. R.; Thapar, N.; Katz, J. E.; Clarke, S.; Yeates, T. O. Crystal Structure of a Protein Repair Methyltransferase from *Pyrococcus furiosus* with its L-Isoaspartyl Peptide Substrate. *J. Mol. Biol.* **2001**, *313*, 1103–1116.

(34) Skordalakes, E.; Dodson, G. G.; Green, D. S.; Goodwin, C. A.; Scully, M. F.; Hudson, H. R.; Kakkar, V. V.; Deadman, J. J. Inhibition of Human α-Thrombin by a Phosphonate Tripeptide Proceeds via a Metastable Pentacoordinated Phosphorus Intermediate. *J. Mol. Biol.* **2001**, *311*, 549–555.

(35) Parry, M. A.; Fernandez-Catalan, C.; Bergner, A.; Huber, R.; Hopfner, K. P.; Schlott, B.; Guhrs, K. H.; Bode, W. The Ternary Microplasmin−Staphylokinase−Microplasmin complex is a Proteinase−Cofactor−Substrate Complex in Action. *Nat. Struct. Biol.* **1998**, *5*, 917–923.

(36) Brandstetter, H.; Kuhne, A.; Bode, W.; Huber, R.; von der Saal, W.; Wirthensohn, K.; Engh, R. A. X-ray Structure of Active Site-Inhibited Clotting Factor Xa. Implications for Drug Design and Substrate Recognition. *J. Biol. Chem.* **1996**, *271*, 29988–29992.

(37) Mueller, M. M.; Sperl, S.; Sturzebecher, J.; Bode, W.; Moroder, L. (*R*)-3-Amidinophenylalanine-Derived Inhibitors of Factor Xa with a Novel Active-Site Binding Mode. *Biol. Chem.* **2002**, *383*, 1185–1191.

(38) Adler, M.; Kochanny, M. J.; Ye, B.; Rumennik, G.; Light, D. R.; Biancalana, S.; Whitlow, M. Crystal Structures of Two Potent Nonamidine Inhibitors Bound to Factor Xa. *Biochemistry* **2002**, *41*, 15514–15523.

(39) Katona, G.; Berglund, G. I.; Hajdu, J.; Graf, L.; Szilagyi, L. Crystal Structure Reveals Basis for the Inhibitor Resistance of Human Brain Trypsin. *J. Mol. Biol.* **2002**, *315*, 1209–1218.

(40) Liebeschuetz, J. W.; Jones, S. D.; Morgan, P. J.; Murray, C. W.; Rimmer, A. D.; Roscoe, J. M.; Waszkowycz, B.; Welsh, P. M.; Wylie, W. A.; Young, S. C.; Martin, H.; Mahler, J.; Brady, L.; Wilkinson, K. PRO_SELECT: Combining Structure-Based Drug Design and Array-Based Chemistry for Rapid Lead Discovery. 2. The Development of a Series of Highly Potent and Selective Factor Xa Inhibitors. *J. Med. Chem.* **2002**, *45*, 1221–1232.

(41) Bertrand, J. A.; Oleksyszyn, J.; Kam, C. M.; Boduszek, B.; Presnell, S.; Plaskon, R. R.; Suddath, F. L.; Powers, J. C.; Williams, L. D. Inhibition of Trypsin and Thrombin by Amino(4-amidinophenyl) methanephosphonate Diphenyl Ester Derivatives: X-ray Structures and Molecular Models. *Biochemistry* **1996**, *35*, 3147–3155.

(42) Flipo, M.; Beghyn, T.; Leroux, V.; Florent, I.; Deprez, B. P.; Deprez-Poulain, R. F. Novel Selective Inhibitors of the Zinc Plasmodial Aminopeptidase PfA-M1 as Potential Antimalarial Agents. *J. Med. Chem.* **2007**, *50*, 1322–1334.

JM700962J